



# Multiphysics analysis of fuel fragmentation, relocation, and dispersal susceptibility—Part 1: Overview and code coupling strategies

Ian Greenquist<sup>\*</sup>, Aaron Wysocki, Jake Hirschhorn<sup>1</sup>, Nathan Capps

Oak Ridge National Laboratory, Oak Ridge, TN, United States



## ARTICLE INFO

**Keywords:**  
FFRD  
High burnup  
Nuclear fuels  
Code coupling  
VERA  
TRACE  
BISON

## ABSTRACT

The US nuclear energy industry is investigating strategies to increase the reactor operating cycle to 24 months, resulting in peak rod average burnups exceeding the current limit of 62 GWD/tU. This increase will in turn increase the probability of fuel fragmentation, relocation, and dispersal (FFRD) in the event of a loss-of-coolant accident (LOCA). This effort couples multiple codes to (1) evaluate full-core power histories for high-burnup fuel operated in a Westinghouse 4-loop pressurized water reactor, (2) model a postulated large-break LOCA, and (3) calculate the mass of fuel susceptible to FFRD. This paper, the first of three describing the work, focuses on code coupling strategies and FFRD susceptibility calculations. The other two companion papers focus on code-specific designs and analyses.

Three codes were used in this work. VERA was used to calculate steady-state power histories, TRACE was used to model the transient thermal hydraulics, and BISON was used to model steady-state and transient fuel performance and cladding failure. Several fuel pulverization models were used to calculate FFRD susceptibility in failed rods. Depending on the cladding failure/fuel pulverization model combination, the core-wide FFRD susceptibility during the postulated LOCA range from 0 to over 5,000 kg.

## 1. Introduction

The US nuclear energy industry is investigating strategies to further reduce the cost of energy production by using its existing fleet of nuclear generating stations. Nuclear power plant operating costs are governed by maintenance, surveillance, outage cost, purchase of fresh fuel assemblies, and efficiency of core design. Material costs are typically beyond the operator's control, but core design optimizations offer potential operational savings. The core design envelope available to operators is constrained by regulatory criteria limiting fuel enrichment to 5%  $^{235}\text{U}$  and safety concerns limiting the peak rod average burnup to 62 GWD/tU. These constraints have led to renewed efforts by the nuclear industry to extend the peak rod average burnup beyond 62 GWD/tU. This effort will likely require additional safety analyses beyond those currently accepted by the US Nuclear Regulatory Commission (NRC). The long-term goal of this work is to demonstrate a best-estimate-plus-uncertainty pin-by-pin high-burnup loss-of-coolant accident (LOCA) analysis technique to assess full-core high-burnup fuel fragmentation, relocation, and dispersal (FFRD) and to identify approaches for minimizing or potentially mitigating FFRD through core design

optimizations.

Historically, the design basis limits for cladding materials were determined by mechanically testing cladding alloys that had been irradiated under normal service condition and subsequent semi-integral LOCA testing to determine the embrittlement thresholds. This effort was further expanded when a limited number of integral tests were performed to identify and evaluate the dominant failure modes. Thus, it was determined that semi-integral or separate effects test data were applicable to the relevant fuel safety limits up to burnups of 62 GWD/tU.

Integral tests using the Halden reactor in Norway—and later semi-integral tests at Studsvik—revealed that the response of high-burnup fuel pellets to LOCA conditions could dramatically change from that seen in previous observations (Capps et al., 2020). Up to ~67 GWD/tU fuel pellets were observed to fragment into pieces that were large compared with the size of the cladding rupture, and large fragments relocating into the balloon region were modest. However, some Halden and Studsvik tests conducted on fuel samples irradiated to >67 GWD/tU showed that fuel pellets could pulverize into small fragments (Capps et al., 2020). A significant fraction of these particles was fine enough to relocate axially within the balloon region and eject through the rupture opening into the coolant. If this behavior were sufficiently significant,

\* Corresponding author.

E-mail address: [greenquistit@ornl.gov](mailto:greenquistit@ornl.gov) (I. Greenquist).

<sup>1</sup> Current affiliation: Idaho National Laboratory, Idaho Falls, ID, United States.

Nomenclature	
AFC	Advanced Fuels Campaign
BEMUSE	Best Estimate Methods—Uncertainty and Sensitivity Evaluation
BU	Burnup
FCT	Fuel centerline temperature
FEM	Finite Element Method
FFRD	Fuel fragmentation, relocation, and dispersal
FGR	Fission gas release
GWd	Gigawatt day
HBFF	High burnup fuel fragmentation
HDF5	Hierarchical data format 5
INL	Idaho National Laboratory
LBLOCA	Large-break loss of coolant accident
LOCA	Loss of coolant accident
LHR	Linear heat rate
LWR	Light water reactor
MOOSE	Multiphysics Object Oriented Simulation Environment
NEAMS	Nuclear Energy Advanced Modeling and Simulation
NRC	Nuclear Regulatory Commission
NQA-1	Nuclear Quality Assurance
OECD	Organisation for Economic Co-operation and Development
ORNL	Oak Ridge National Laboratory
PCT	Peak cladding temperature
PWR	Pressurized water reactor
RIL	Research information letter
RIP	Rod internal pressure
TH	Thermal hydraulic
TRACE	TRAC/RELAP Advanced Computational Engine
tU	Ton of uranium
VERA	Virtual Environment for Reactor Applications

then it could invalidate historical approaches used to demonstrate safety and the effect of FFRD, specifically assumptions related to core coolability and criticality.

This work builds on previously developed methodologies (Capps et al., 2020; Capps et al., 2020; Capps et al., 2021) to evaluate core-wide FFRD susceptibility. This work assesses important steady-state operational and fuel performance parameters that are known to contribute to FFRD susceptibility. The parameters are evaluated to support future high-burnup LOCA test plans and to inform core design strategies that reduce or potentially mitigate FFRD. Additionally, a subset of high-burnup fuel rod data representing the high-burnup operation envelope will be passed to the TRAC/RELAP Advanced Computational Engine (TRACE) for detailed thermal-hydraulic (TH) evaluation and subsequently to BISON for transient fuel performance analysis. The results from this study will be used to inform semi- and fully integral LOCA tests programs, determine cladding rupture susceptibility and those parameters that increase it, and FFRD susceptibility if rupture is predicted. Again, the long-term goal of this work is to demonstrate a best-estimate-plus-uncertainty methodology to assess core-wide FFRD susceptibility and to inform high-burnup core design approaches intended to minimize or potentially mitigate FFRD susceptibility.

The commercial pressurized water reactor (PWR) chosen for this analysis is a Westinghouse four-loop plant with an ambient pressure containment design, a capacity of 193 nuclear fuel assemblies, and a rated power of 3,626 MW<sub>th</sub>. Current fuel management strategies for the PWR employ 18-month fuel cycle designs. However, a transition scheme to a 24-month cycle design was modeled by Southern Nuclear Company and Oak Ridge National Laboratory (ORNL) (Capps et al., 2020; Capps et al., 2021). The design utilizes fresh fuel, once-burned fuel, and twice-burned fuel. The twice-burned fuel is always placed on the core's periphery, where power ratings and temperatures are lowest. A methodology was developed to characterize the operating conditions and fuel performance of high-burnup fuel rods during both steady-state operations and during a postulated large-break LOCA (LBLOCA). First, the Virtual Environment for Reactor Applications (VERA) was used to model the transition from an 18-month fuel cycle to a 24-month fuel cycle, followed by steady-state 24-month operating cycles for the full reactor core. VERA calculated the power and temperature histories of every rod in the core. A statistically representative subset of rods was selected and modeled using the finite element method (FEM)-based fuel performance code BISON. VERA results were used as the initial conditions for a steady state fuel performance simulation using BISON as well as a steady-state TH simulation using TRACE. The results of both simulations were compared to ensure accuracy. Then a transient LBLOCA simulation was performed using TRACE. TRACE predictions were used as boundary conditions for a second set of BISON simulations predicting fuel

performance during the LBLOCA. A statistical analysis of these BISON results was performed to predict the full-core susceptibility to FFRD during an LBLOCA event. The passage of information between the various sets of simulations is diagrammed in Fig. 1.

This paper is the first of three describing the complete work. This paper focuses on code coupling and the FFRD analysis. Part two describes the steady state fuel performance calculations and sensitivity study (Capps et al.). Part three provides a detailed description of the thermal hydraulics model (Wysocki et al., Unpublished manuscript).

## 2. Vera full-core simulations

VERA is a high-fidelity multiphysics simulation environment capable of simulating a full light-water reactor (LWR) core down to individual fuel rods. It includes physics modules for neutron transport, thermal hydraulics, fuel performance, and chemistry (Turner et al., 2016). A previously-published VERA model was used in the present work to establish realistic irradiation and temperature histories for the fuel rods, including the effects of reshuffling (Capps et al., 2020). These histories were used to inform steady-state fuel performance models of individual fuel rods. VERA was the only code used to model the neutron transport of the fuel rods.

### 2.1. Simulation setup

VERA simulation results are stored as hierarchical data format 5 (HDF5) files. Each HDF5 file contains the operating conditions needed to reconstruct fuel rod irradiation histories for one cycle. Fourteen HDF5 files were available for the high-burnup VERA core designs introduced in Section 2. These included two cycles during which the core transitioned from using standard-burnup (<62 GWd/tU) fuel rods to high-burnup fuel rods, nine cycles during which the core had not yet achieved equilibrium behavior, and three cycles during which the core operated at equilibrium. The following sections describe operating conditions of interest, the process applied to down-select cycles for further analysis, high-burnup operating conditions in the selected cycles, and the process applied to down-select fuel rods for fuel performance analysis.

Rod conditions of interest were selected to assess the susceptibility of high-burnup fuel rods to FFRD. Selections were based on the previously published high-burnup fuel fragmentation (HBFF) analysis methodology (Capps et al., 2020) shown in Fig. 2. It considers spatial variations in burnup, temperature, and cladding ballooning. Only positions where burnup, temperature, and cladding ballooning conditions are met are considered as susceptible to FFRD. Operating conditions are compared with criteria established for each parameter to develop a composite

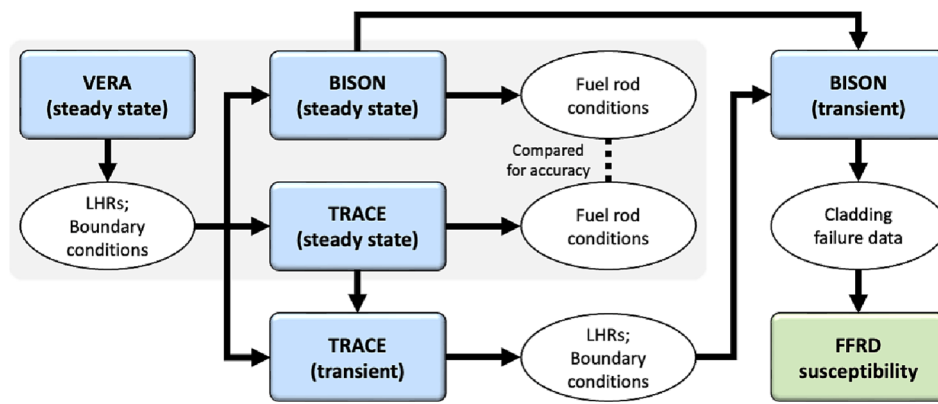


**Fig. 1.** Flow chart of the passing of data between codes used in this work. Blue boxes represent codes and white ovals represent data passed between codes. The green box represents the calculation of FFRD susceptibility. The steady state steps are all in the gray region.

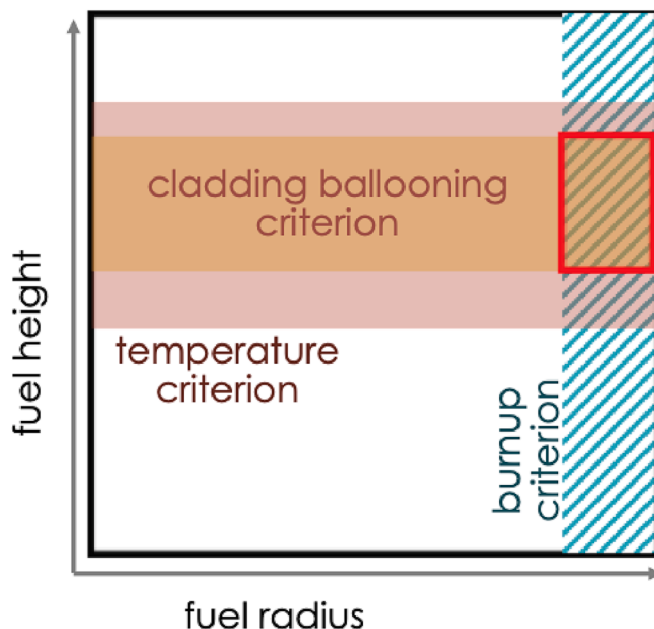


**Fig. 2.** Diagram illustrating the local burnup, fuel temperature, and cladding ballooning criteria that factor into FFRD susceptibility. The fuel within the red rectangle meets all three criteria and is therefore believed to be susceptible to FFRD. Modified from Capps et al. (Capps et al., 2020).

criterion that estimates the mass of fuel susceptible to fragmentation and subsequent dispersal under LBLOCA conditions. The methodology was leveraged to identify operating conditions of interest within the VERA HDF5 files. Selections were made to characterize fuel rod temperature behaviors, burnup behaviors, and the spatial relationships between them. Nine operating conditions of interest were defined:

1. Average fuel rod burnup
2. Average fuel rod linear heat rate (LHR)
3. Average fuel rod decay heat production rate
4. Peak fuel rod burnup
5. Axial location of the peak fuel rod burnup
6. Local LHR at the axial location of the peak fuel rod burnup
7. Peak fuel rod LHR
8. Axial location of the peak fuel rod LHR
9. Local burnup at the axial location of the peak fuel rod LHR

Three aspects of these nine operating conditions require further discussion. First, LHRs were selected as surrogates to characterize fuel

rod temperature behaviors. Fuel rod temperature estimates calculated by VERA's TH module, CTF (Salko et al., 2020), are available in the HDF5 files. However, BISON temperatures are considered higher fidelity because BISON includes additional physical effects like fission gas release (FGR) and rod internal pressure (RIP). Therefore, BISON was used to calculate all rod temperatures in this work. Fuel rod temperature behaviors are analyzed directly via BISON fuel performance simulations, which are discussed in Section 3.

Second, decay heat production rates were assumed to be 9.5% of the LHRs according to an approximation given in El-Wakil (El-Wakil, 1978). VERA calculates irradiation history-dependent decay heat production rates using its isotope depletion, decay, and activation module, ORIGEN (Rearden and Jessee, 2018). However, these calculations were not implemented in the high-burnup VERA core designs being examined here. Therefore, the LHR-based approximation was determined to be sufficient for the purposes of cycle and fuel rod down-selection in the current work. Future work may attempt to incorporate decay heat production rates.

Finally, VERA did not calculate radially discretized burnups or LHRs within individual fuel rods for this work. Examining these operating conditions helps to assess the combined effects of burnup and temperature in accordance with the HBFF analysis methodology illustrated in Fig. 2. The third HBFF-relevant behavior, cladding ballooning, is analyzed via BISON fuel performance simulations, which are discussed in Section 3.

## 2.2. Simulation Results

The steady-state fuel rods were filtered to eliminate those that did not achieve a rod average burnup of 62 GWD/tU by the end of three cycles. Existing operational and safety limits were assumed to be adequate to address undesirable fuel performance behaviors in fuel rods with average burnups of less than 62 GWD/tU. Therefore, standard-burnup fuel rods were not considered further in this work. Fuel rods inserted into the reactor before the first steady-state cycle were also filtered out, yielding 32,944 complete high-burnup fuel rod histories.

Time-dependent operating conditions are plotted for the remaining high-burnup fuel rods in Fig. 3. Note that the three cycles modeled are labeled as 28, 29, and 30 in the VERA simulation and that the opacities of the data have been adjusted to display overlapping data more clearly. The plots illustrate how the operating conditions for this population of fuel rods evolve within each cycle and from one cycle to another. The results in Plots 3B, 3F, and 3G show that, at any given time, LHRs vary widely between fuel rods. This behavior is primarily attributed to the fuel rods being irradiated in different locations throughout the core but could also be attributed in part to burnable poisons. Assembly shuffling between cycles produces additional complexities. Plots 3A, 3D, 3I show that these spatial variations in LHR cause fuel rods to accumulate

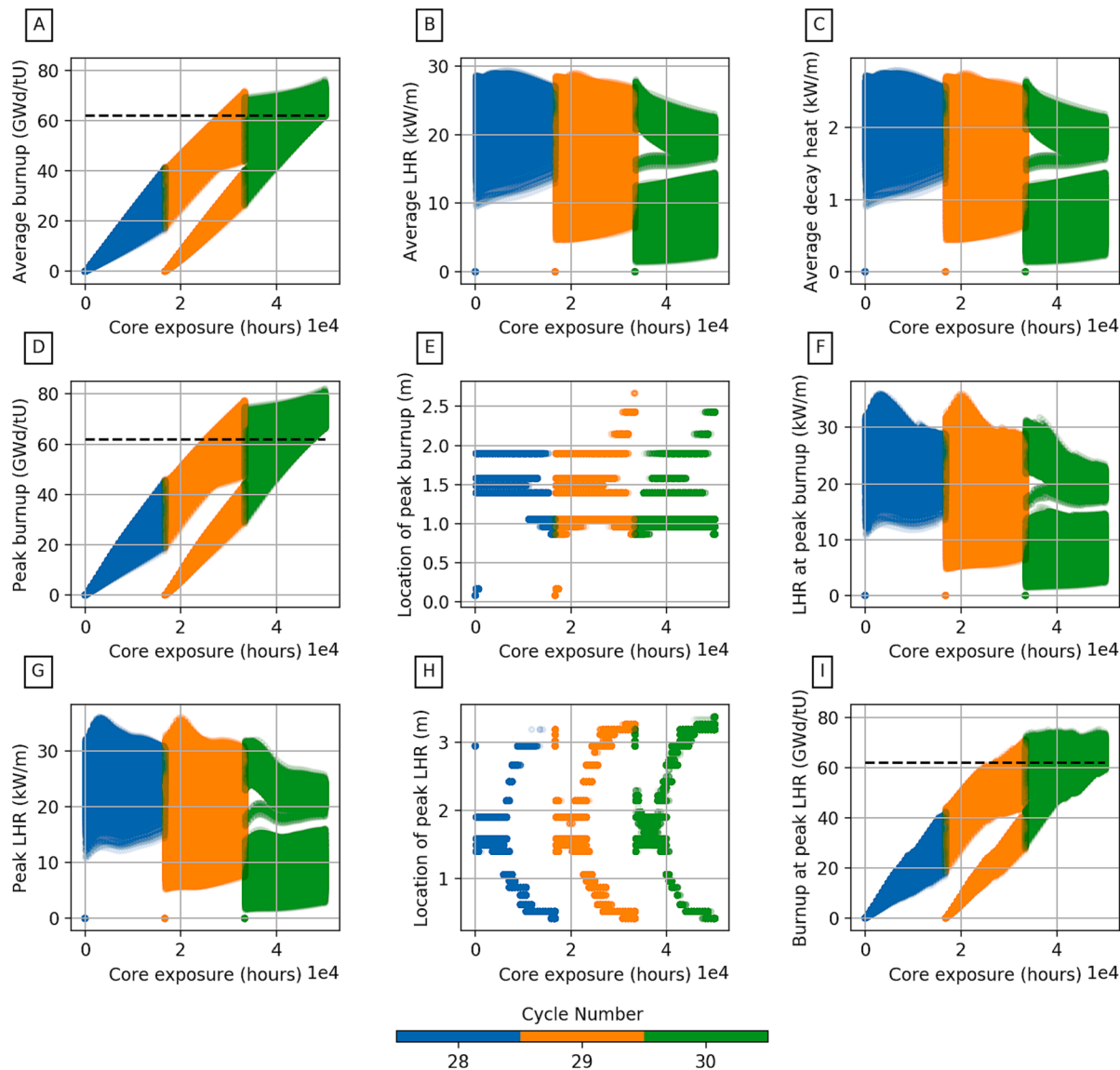


**Fig. 3.** Time-dependent operating conditions extracted from 32,944 fuel rods irradiated in steady-state operating cycles. Fuel rods irradiated in previous cycles and those that did not achieve an average burnup of at least 62 GWD/tU (marked by the dashed lines in A, D, and I) are not shown. The plots show that fuel rods experience wide ranges of operating conditions, which vary with fuel rod location and time.

burnup at different rates. These observations suggest that susceptibility to FFRD may vary spatially throughout the core and over time.

The axial locations of the peak burnup shown in Plot 3E and peak LHR shown in Plot 3H exhibit several features that warrant further discussion. Both plots reveal the axial discretization applied in the VERA simulations, which produced 49 axial regions. This level of axial discretization was considered sufficient for the purposes of characterizing steady-state operating conditions in this work. Plot 3E shows that the axial location of the peak burnup lies near the midplane for most fuel rods. This accelerates fuel burnup near the midplane, which depresses local LHR later in fuel life. Plot 3H shows how the axial location of the peak LHR evolves over time. The axial location of the peak LHR in each fuel rod shifts from the midplane toward the top or bottom of the fuel rod, depending on its irradiation history and location in the core.

Additional analyses were also performed on the VERA simulation results. These include statistical analyses, fuel rod operating condition distributions, and time-of-peak-value distributions for each operating cycle. The results are included in Part 2 of this paper series. The purpose of this paper is to discuss how these results were used to inform the subsequent BISON analysis.

### 3. Bison steady-state simulations

BISON is a FEM-based fuel performance code maintained by Idaho National Laboratory (Williamson et al., 2021) (INL). It is built on the Multiphysics Object Oriented Simulation Environment (MOOSE), also maintained by INL. BISON maintains all of MOOSE's functionality as well as fuel-performance-specific capabilities. BISON is well validated and Nuclear Quality Assurance (NQA-1) certified to simulate LWR fuels and claddings. It includes models to predict heat transfer, fuel swelling and other strains, fuel-cladding interactions, fission gas generation and release, and other effects. This section gives a brief overview of the BISON model and results. A complete description is provided in Part 2 of this work (Capps et al.).

BISON simulations were generated based on the VERA predictions shown above and used to predict the steady-state fuel performance of individual rods. These results were used to benchmark TH simulations of a postulated LOCA.

### 3.1. Simulation setup

VERA simulations like those used to produce the results being examined in the current work take approximately 24 h per cycle to run on 1,000 cores. A BISON simulation for one fuel rod with a three-cycle irradiation history takes approximately 3 h to run on 16 cores on INL's Sawtooth cluster (Intel Xeon 8268 CPUs with 192 GB of RAM). The benefits of parallelization when simulating one fuel rod in BISON diminish as more cores are added, but the number of fuel rods that can be simulated in parallel is limited only by cluster availability and utilization limits. Although these values are approximate, they can be used to estimate the magnitude of the time and computational resources needed to simulate high-burnup fuel rods in BISON.

Assuming that BISON simulations are run with 16 cores each and that total cluster usage is limited to 1,000 cores total, it would take approximately 1,581 h (66 days) to run all 32,944 high-burnup fuel rods identified in cycles 28–30. Furthermore, the BISON simulations were expected to need to run multiple times for each fuel rod to enable troubleshooting and provide support for follow-on TH and transient analyses as needed. Additionally, industry application of this methodology may require simulation of multiple cores to optimize the core design. This could result in an order of magnitude increase in run time. For these reasons, a smaller subset of fuel rods representative of the core-wide behavior was selected for BISON fuel performance analysis.

The method used to downselect a statistically representative sample of fuel rods is explained in more detail in Part 2 of this paper series. At this writing, it is sufficient to say that 753 rods were selected for steady-state BISON simulations, distributions of predicted values for the 753 rods were similar to those of the 32,944 rods, and the statistical values for the 753 rods matched the same values for the 32,944 rods within  $\pm 2\%$ .

Six parameters of interest were identified for the BISON simulations:

1. RIP
2. FGR
3. Peak fuel centerline temperature (FCT)
4. Axial location of peak FCT
5. Radial-averaged burnup at the location of peak FCT
6. LHR at the location of peak FCT

### 3.2. Simulation results

The six parameters of interest are plotted against both average burnup and average LHR in Fig. 4. Note that the cycles (and therefore colors) in the plots overlap because the fuel performance parameters are plotted against average burnup and average LHR rather than time. The opacities of the data have been adjusted to show the overlapping cycles more clearly and to better illustrate the overall trends. The RIP and FGR predictions in Plots 4A and 4B, respectively, correlate well with average burnup and exhibit the expected behaviors. The peak FCT predictions in Plots 4C and 4I show that peak FCT is correlated more strongly with average LHR than with average burnup. These relationships suggest that FFRD-relevant parameters depend not only on the fuel rod burnup, but also on the way that fuel rods with various burnups are operated (i.e., LHRs, LHR histories, and temperatures). Finally, these results will be used to inform subsequent high-burnup LOCA testing, high-burnup TRACE analysis, and BISON transient analysis. A more detailed analysis of the BISON core-wide results is presented in Part 2 of this paper series.

## 4. Trace LBLOCA simulations

TRACE is a best estimate reactor systems code developed and maintained by the NRC. It combines the capabilities of multiple NRC systems codes (Bajorek et al., 2022). TRACE is specifically designed to model large break and small break LOCAs and other accident scenarios

for LWRs with a specific emphasis on the hot rod. It includes models for multidimensional two-phase flow, nonequilibrium thermodynamics, heat transfer, reflood, level tracking, and reactor kinetics.

TRACE was used to model a postulated LOCA. The previous BISON simulations were used to inform the modeling assumptions, and the results provided transient TH boundary conditions for additional BISON simulations of the accident. This section gives a summary of the simulation and setup. A more complete description is provided in Part 3 of this work (Wysocki et al., Unpublished manuscript).

### 4.1. Simulation setup

The starting point for the TRACE analysis was a preexisting TRACE model based on the Zion nuclear power plant, a Westinghouse 4-loop PWR. The model was provided to users as part of the TRACE code distribution and was chosen as a starting point for the Best Estimate Methods—Uncertainty and Sensitivity Evaluation (BEMUSE) Organisation for Economic Co-operation and Development (OECD) International Benchmark conducted in the late 2000 s to simulate a realistic LBLOCA event in PWRs (Reventos et al., 2008). Only the best-estimate portion of the model was used for this work. Sensitivity and uncertainty analysis is planned for future work.

The present study implemented several changes to the preexisting TRACE model in accordance with the recommendations provided in the BEMUSE benchmark specifications. These modifications, described in detail in Part 3 of this paper series, improved the fidelity and representativeness of the model for simulating PWR LBLOCA. As shown in Part 3, the current TRACE model provides good agreement with the results calculated by the BEMUSE benchmark participants using several different systems codes.

The current TRACE model employed a similar core modeling approach as that recommended by BEMUSE. The fuel rods in the core were grouped into three TRACE “heat structure” components: a high-burnup rod of interest, the assembly containing that rod, and the remainder of the core. The flow channels in the core were similarly grouped into three TRACE “pipe” components, corresponding to the flow surrounding the rods within each of the three heat structure components. A separate TRACE calculation was performed for each of 281 high-burnup rods of interest. Sections 2 and 3 identify 753 high-burnup rods of interest across cycles 28–30, of which 281 were present in cycle 30 and had BISON results available at the end of the cycle.

Core inlet temperature, inlet flow rate, and outlet pressure were applied to the TRACE model consistent with the cycle design presented in Section 2. These conditions were taken from the end of the cycle, which provides the highest rod burnups and likely the greatest mass of fuel susceptible to FFRD. The VERA 3D power and burnup distributions from the reference high-burnup cycle were averaged onto these TRACE grouped rods to produce an axial-dependent power and burnup profile for each grouped rod. The resulting 281 TRACE calculations were simultaneously executed on INL's Sawtooth high performance computing platform, with the longest case requiring 20 h of wall time to complete.

### 4.2. Simulation results

The distribution of rod-averaged burnup and LHR for the 281 high-burnup rods is presented in Fig. 5. The term “reload number” indicates the number of previous irradiation cycles for which a given fuel rod and its assembly have been in the core. All the twice-irradiated high-burnup rods are located at the periphery of the core, leading to rod-averaged LHR values lower than those for the once-irradiated assemblies in the core interior. Although this leads to lower transient cladding temperatures in the twice-irradiated assemblies, their higher burnup level necessitates their inclusion in the transient FFRD analysis.

The time-dependent peak cladding temperature (PCT) results for all 281 high-burnup rods are shown in Figs. 6 and 7. As expected, the

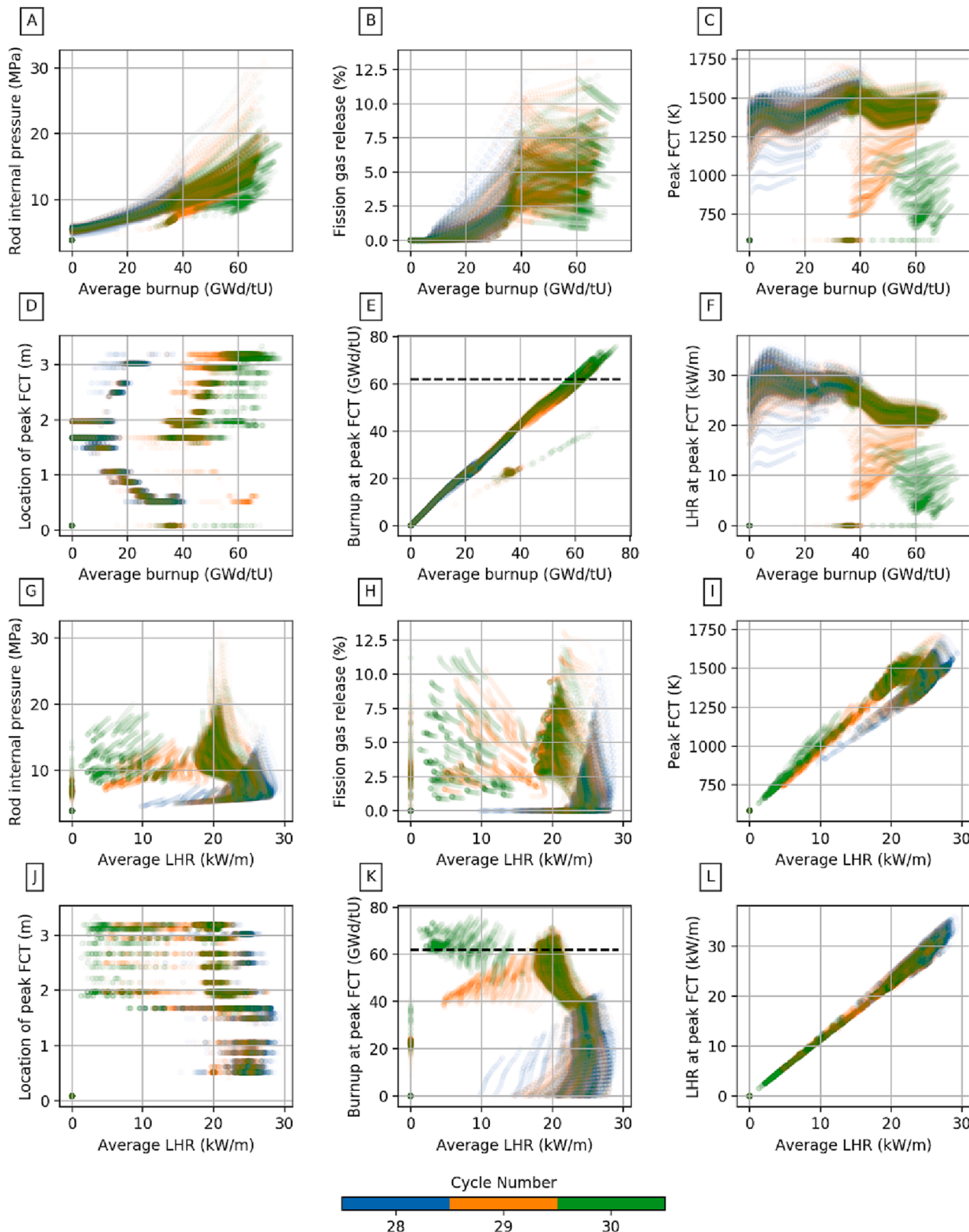


**Fig. 4.** Average burnup- and LHR-dependent fuel performance results extracted from the 753 fuel rods selected for analysis in BISON. Opacity is adjusted to show data that overlap in burnup- and LHR-space more clearly. Plots A–C show that the fuel rods exhibit a wide range of responses to irradiation. Plots D–L begin to illustrate correlations among the fuel performance results and the operating conditions examined in Section 2.

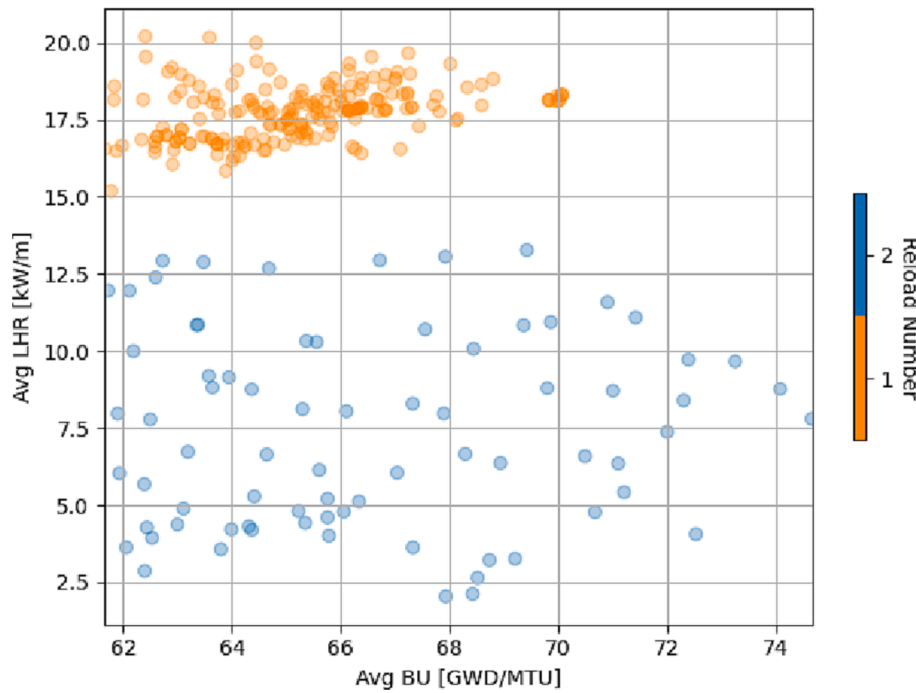


Fig. 5. Rod-averaged burnup and LHR for the 281 high-burnup rods.

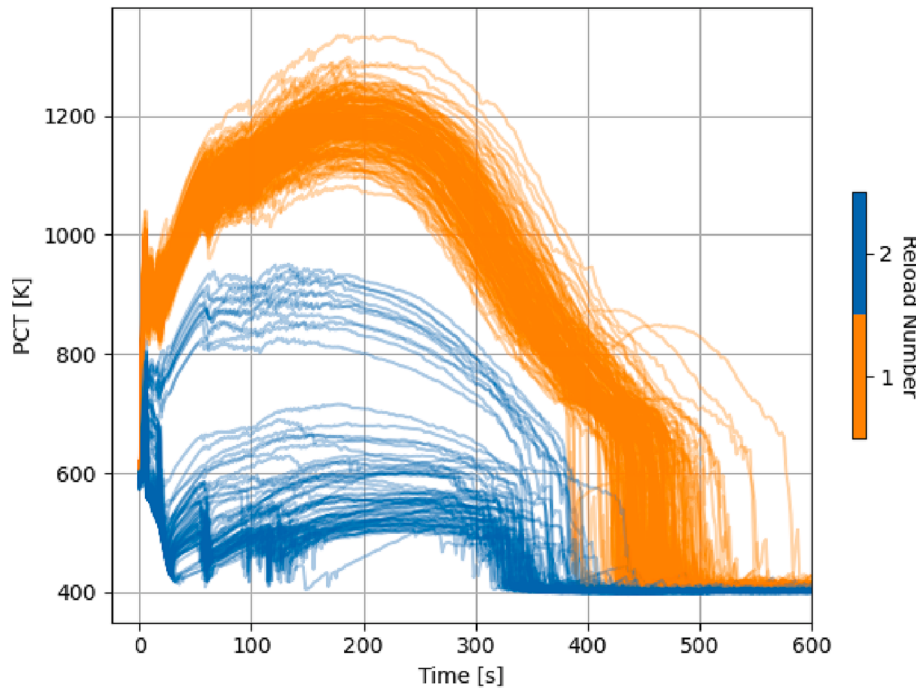


Fig. 6. LBLOCA PCT vs. time for the 281 high-burnup rods.

cladding temperatures increased rapidly within the first 5 s after the break as a result of impaired core cooling and large stored energy in the fuel rods. Over the next several minutes, the cladding heated more slowly because of continued decay heat production until quenching of the fuel rod hot spot occurred.

In addition, the coolant system pressure for the first 150 s of the LBLOCA is shown in Fig. 8. The pressure dropped from the steady-state operating pressure of 15.7 MPa to 0.2 MPa within 30 s, which corresponds to the blowdown phase of the LOCA. The pressure remained at 0.2 MPa for the remainder of the transient.

An additional TRACE run (not shown) was performed for the rod with the highest overall LHR in the core regardless of burnup. This case gave a PCT of 1,413 K, compared to PCTs of 609 K to 1,335 K for the high-burnup rods. LOCA analyses performed under existing NRC safety guidelines would compare the maximum PCT for the single hottest rod in the core against the 1,478 K cladding temperature limit defined by 10 CFR 50.46 (Nrc, 2021). Although the high-burnup rods exhibited lower PCT values than those exhibited by the peak power rod, the combination of elevated PCT and high-burnup levels necessitates detailed fuel performance evaluation of these high-burnup rods to assess their FFRD

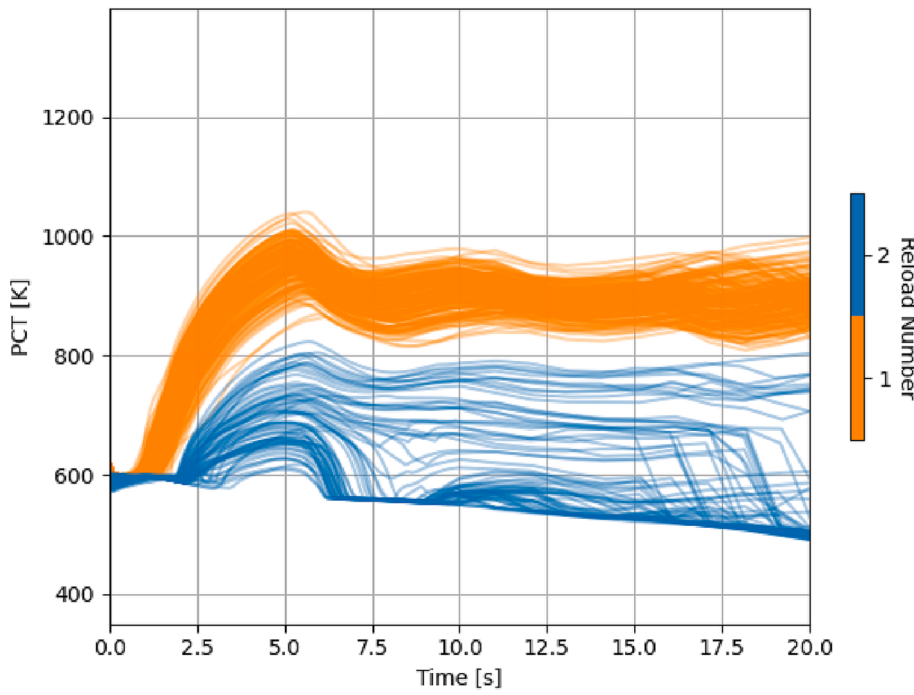


Fig. 7. LBLOCA PCT vs. time for the 281 high-burnup rods ( $t = 0$  to 20 sec).

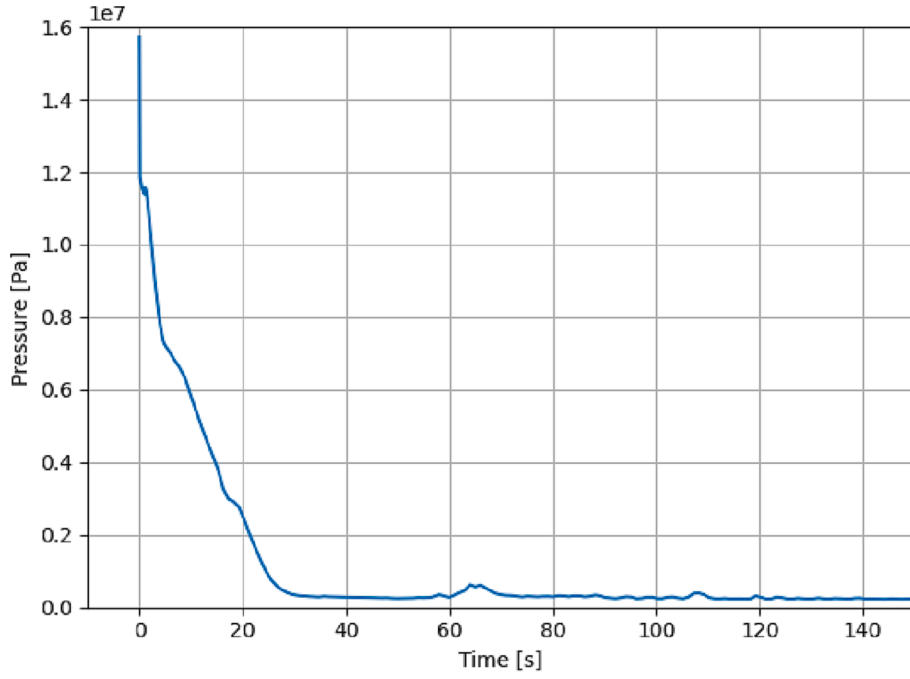


Fig. 8. Coolant system pressure for the first 150 s of the LBLOCA.

susceptibility.

## 5. Bison LBLOCA simulations

The TRACE predictions presented above were used to inform the irradiation and thermal boundary conditions of transient BISON simulations. The BISON simulations were designed to predict cladding failure (i.e., rupture) using preexisting cladding failure models. The results of the transient BISON simulations were used to calculate the core-wide FFRD susceptibility.

### 5.1. Simulation setup

BISON was used to predict the thermomechanical fuel and cladding performance of the 281 high-burnup rods simulated in TRACE under LBLOCA conditions. The steady-state BISON input files for the 281 rods were used as a starting point. System response data from TRACE were added to evaluate fuel performance under LBLOCA conditions. Therefore, each BISON simulation included both the steady-state and LBLOCA conditions. The rod-average LHRs, axial peaking factors, cladding surface temperatures, and system pressure were received from the VERA

and TRACE results and applied to the final full-power time step and boundary conditions using a custom Python script. The script also added additional materials, postprocessors, vector-postprocessors, and cladding failure models needed to predict cladding failure and analyze LBLOCA conditions. These changes will be discussed in more detail in a subsequent paper.

FEM does not allow the mesh to break apart as it would if the cladding ruptured. Rather, BISON implements three failure criteria that are available from the literature (Powers and Meyer, 1980; Erbacher et al., 1982; Di Marcello et al., 2014). Two were used to evaluate the rods for this case: the strain rate criterion, in which the rod has failed if the rate of change of the cladding hoop strain exceeds  $100 \text{ h}^{-1}$  (Di Marcello et al., 2014), and the Chapman correlation, in which the rod has failed if the cladding temperature exceeds a burst temperature based on an empirical correlation of hoop stress and cladding heating rate (Powers and Meyer, 1980; Erbacher et al., 1982). Note that the correlation between burst temperature and cladding heating rate is positive, such that lower heating rates result in lower burst temperatures.

## 5.2. Simulation results

Of the 281 rod simulations, 35 crashed before reaching the transient, and an additional four crashed within 1 s of the transient start, leaving 242 rods: 64 twice-burned rods and 178 once-burned rods. The cause of the crashes is not clear, and the crashes appear to be randomly distributed. Each simulation was allowed to continue until it either reached a transient time of 600 s, the hoop strain exceeded 100%, it crashed, or it exceeded a wall time of seven days. The fuel rod transient results are shown in Fig. 9. Plots 9A and 9B show the decay heat in terms of LHR and PCT for each rod, respectively. These values were boundary conditions based on TRACE results. Plots 9C and 9D show the peak fuel surface and centerline temperatures, respectively. Plot 9E shows the plenum pressure, and Plot 9F shows the peak cladding hoop strain. In every case, the behaviors of the once-burned rods (cycle 29) are drastically different compared with the twice-burned rods (cycle 28). In addition, none of the simulations of once-burned rods finished. The majority crashed upon reaching a peak hoop strain of 72–74% because of plastic instability-induced deformations in their meshes. Another

important feature to highlight is the convergence of the fuel centerline and fuel periphery temperatures. Fuel centerline temperature for all simulations (once- and twice-burned) decreased from the initial steady-state full-power conditions at the onset of the transient. Surface temperatures for the once-burned fuel rods increased at a rate similar to the decrease rate of the centerline temperatures, and eventually the two temperatures converged, resulting in a nearly flat temperature profile. The twice-burned fuel rods show an initial decrease of both the fuel centerline and periphery temperatures before increasing again.

In addition to the transient behaviors shown in Fig. 9, the pre-transient conditions of each rod are also important. Therefore, the distributions of the pretransient conditions are shown in Fig. 10. Similar to Fig. 5, it shows that the once- and twice-burned rods were operating in very different conditions. Plot 10A shows that the LHRs of the two sets of rods had no overlap. Plots 10B, 10C, and 10D show there was likewise no overlap in the rod temperature profiles. However, Plots 10E and 10F show there was some overlap in plenum pressure and significant overlap in the peak hoop strain, respectively.

Two models were implemented in the BISON simulations to determine if, when, and where cladding failure occurred: the Chapman correlation and the strain rate criterion. The Chapman correlation predicted 182 rod failures: 177 once-burned rods and five twice-burned rods. The strain rate criterion predicted all 178 once-burned rods and none of the twice-burned rods would burst. The predictions in Fig. 9 were plotted again in Fig. 11 and colored based on whether the Chapman correlation predicted failure. The one once-burned rod that did not fail had the lowest fuel temperature. The five twice-burned rods that failed were among those with the highest plenum pressures.

To get a better picture of the relationship between steady-state operating conditions and the likelihood of rod failure, the distributions of pretransient conditions for both failed and nonfailed rods are shown in Figs. 12 and 13. Fig. 12 shows the distributions for once-burned rods, whereas Fig. 13 shows the distributions for twice-burned rods. The six predictions shown match those shown in Figs. 9, 10, and 11. The sole once-burned rod that did not fail had the lowest pretransient LHR, peak cladding temperature, and peak fuel centerline temperature of any once-burned rod. This result suggests that higher LHRs increase the probability of cladding failure. The twice-burned rods

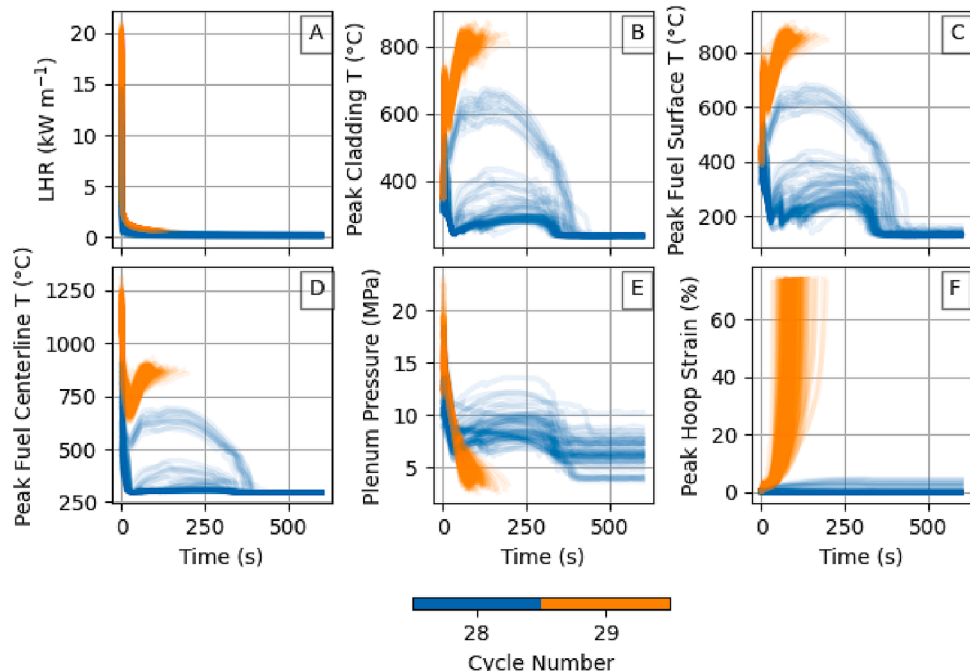


**Fig. 9.** BISON predictions of fuel and cladding performance of 242 high-burnup rods during the LBLOCA transient. Lines are colored according to the number of cycles each rod had been in the core according to the VERA cycle numbers.

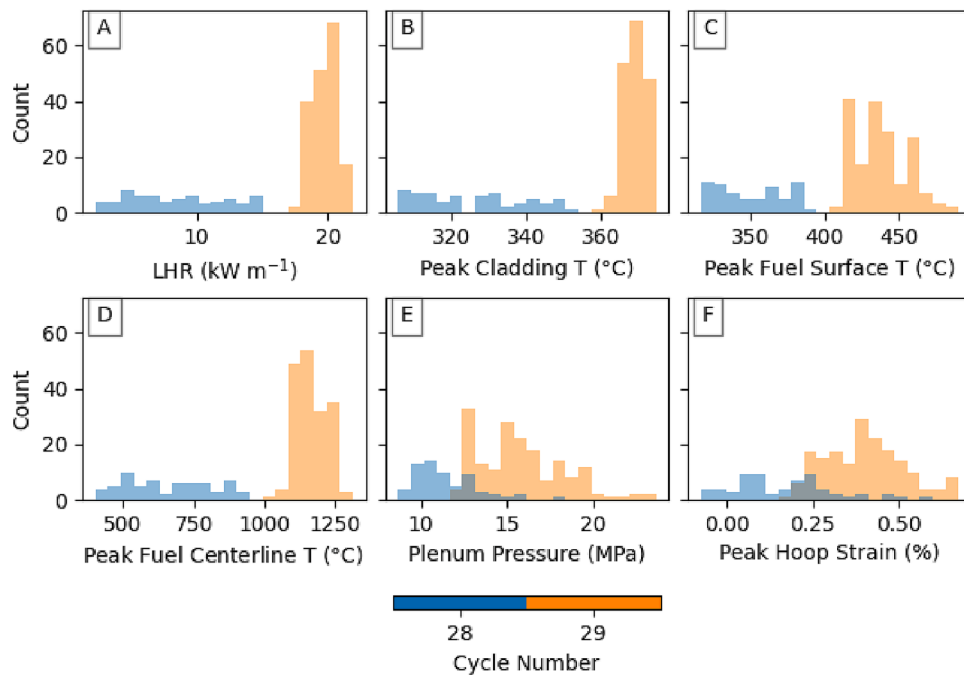


**Fig. 10.** Distributions of pretransient conditions for both once- and twice-burned fuel rods. The conditions shown are (A) LHR, (B) peak cladding temperature, (C) peak fuel surface temperature, (D) peak fuel centerline temperature, (E) plenum pressure, and (F) hoop strain.

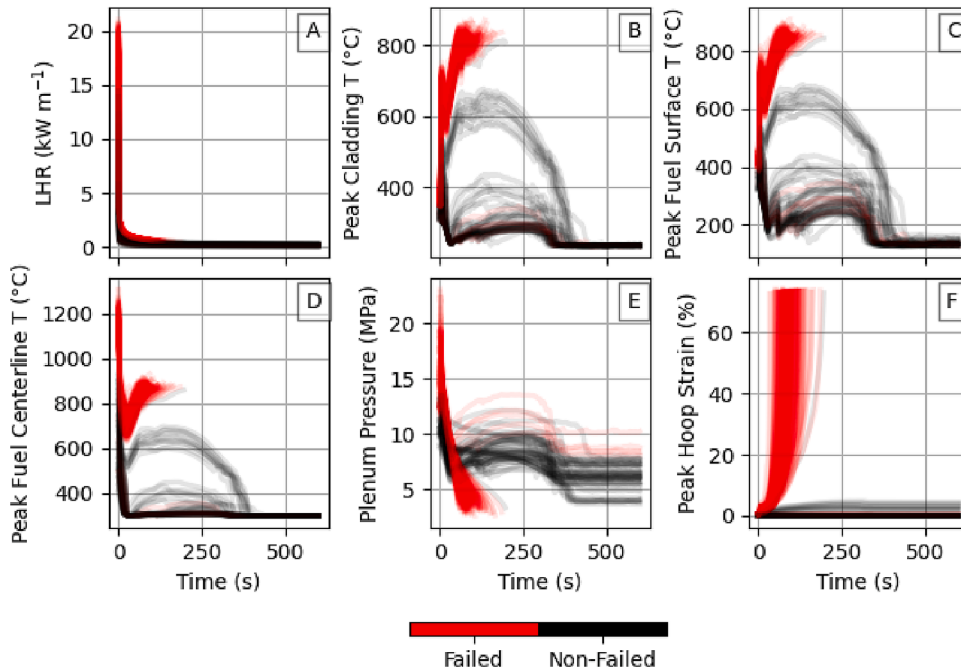


**Fig. 11.** BISON predictions of fuel and cladding performance of 242 high-burnup rods during the LBLOCA transient. Lines are colored based on whether the Chapman correlation predicted cladding burst.

that the Chapman correlation predicted would fail were relatively uniformly distributed among the LHR and temperature profiles. However, Plots 13E and 13F show they had some of the highest pretransient plenum pressures and hoop strains. This suggests that high plenum pressure can lead to high hoop strain, which can lead to cladding failure, even when the LHR and temperature profiles appear to be reasonable.

Note that the single once-burned rod that the Chapman correlation predicted would not fail may have failed if the simulation had reached its peak temperature before crashing. Therefore, some uncertainty exists

in that result. However, this uncertainty is likely smaller than the inherent uncertainty of the model. All the once-burned rods that were simulated did reach their peak temperatures, so no additional failures would likely have been reported among the twice-burned rods.

## 6. Calculation of FFRD susceptibility

The results above form the foundation for predicting the amount of fuel susceptible to dispersion into the reactor pressure vessels using

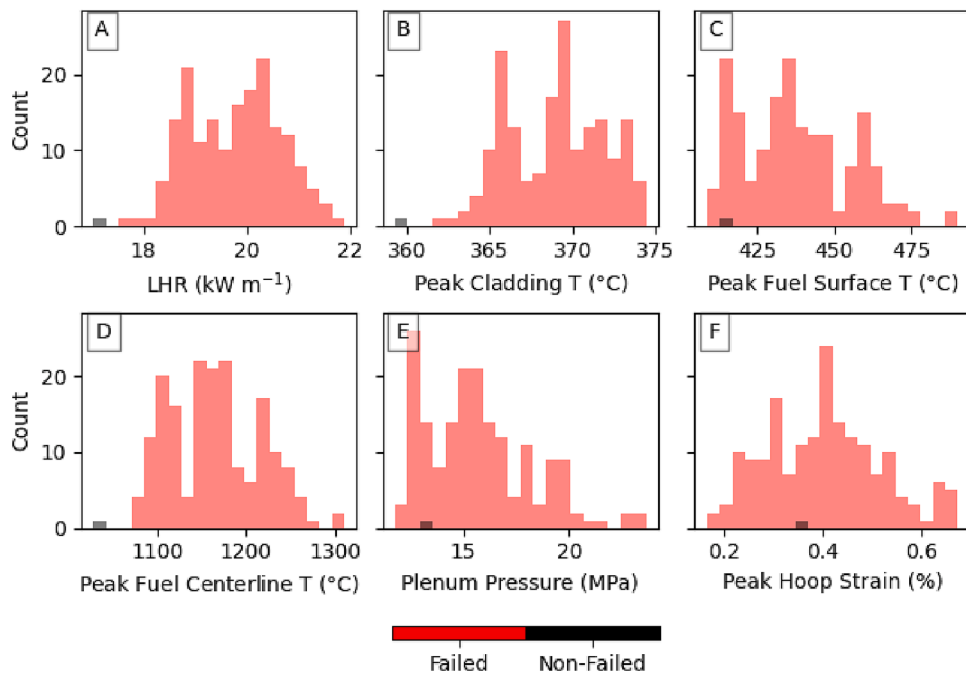


**Fig. 12.** Distribution of pretransient (A) LHR, (B) peak cladding temperature, (C) peak fuel surface temperature, (D) peak fuel centerline temperature, (E) plenum pressure, and (F) hoop strain for both failed and non-failed once-burned rods according to the Chapman correlation.

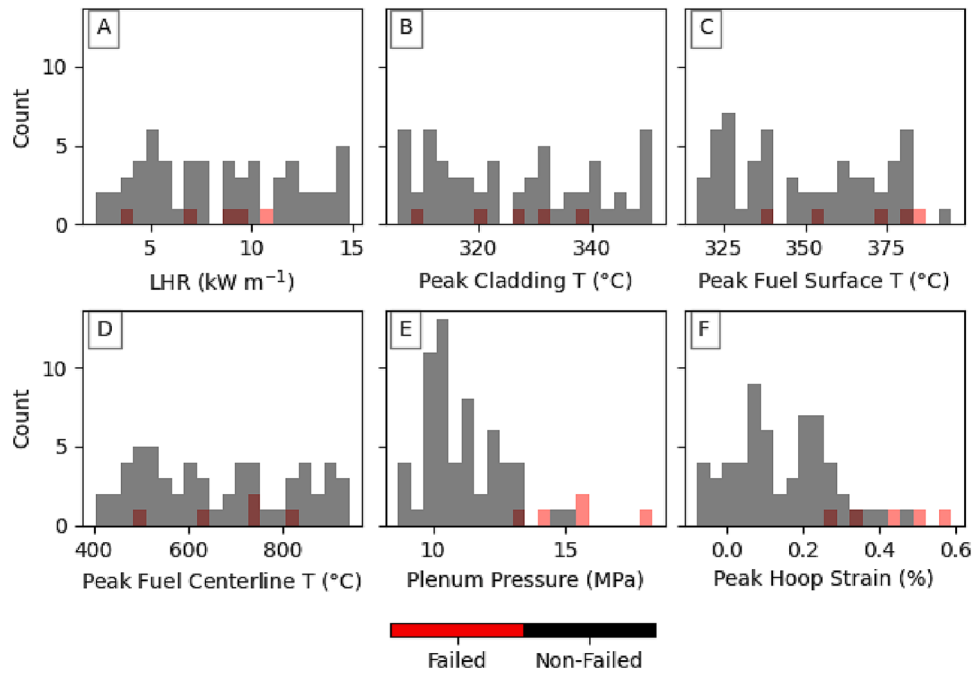


**Fig. 13.** Distribution of pretransient (A) LHR, (B) peak cladding temperature, (C) peak fuel surface temperature, (D) peak fuel centerline temperature, (E) plenum pressure, and (F) peak hoop strain for both failed and non-failed twice-burned rods according to the Chapman correlation.

correlations relating the fuel conditions to pulverization susceptibility. The procedure is as follows. First, determine the axial location where failure occurred using the cladding failure thresholds previously discussed. Second, determine the length susceptible to FFRD per the hoop strain threshold reported in NRC Research Information Letter (RIL) 2021-13 (Bales et al., 2021). However, this work assumes the mixing veins and grid spacers will restrict FFRD to axial positions between the assembly structural components. Future work will investigate the validity of this assumption. Finally, estimate the mass susceptible to pulverization using correlations documented in the NRC RIL (Bales et al.,

2021) or the Turnbull pulverization model (Turnbull et al., 2015). The NRC RIL proposes two correlations for two different fragment sizes. The two correlations consider fragment sizes for particles less than 1 mm and less than 2 mm; both are functions of burnup. Both correlations take the form of Eq. (1) where  $f$  is the fraction of fuel that is susceptible to pulverization,  $a$  is 0.04 and 0.05 in the 1 mm and 2 mm correlations, respectively,  $BU$  is burnup (GWD/tU), and  $C$  is 75 GWD/tU and 80 GWD/tU in the 1 mm and 2 mm correlations, respectively.

$$f = \begin{cases} 0, & BU \leq 55 \\ a(BU - 55), & 55 < BU < C \\ 1, & BU \geq C \end{cases} \quad (1)$$

Whereas the NRC RIL thresholds calculate the mass susceptible to pulverization based on burnup only, the Turnbull correlation utilizes a series of threshold curves to predict the fraction of fuel pulverization based on temperature and burnup. All three models were applied to the cladding failure predictions of both the Chapman correlation and the strain rate criterion.

Fuel rods were broken into regions based on spacer positions. The failure positions of each rod analyzed in Section 5.2 were sorted based on region. The average temperature and burnup of each region that had at least one cladding failure were calculated based on the TRACE predictions. These values were used as the inputs for the fuel pulverization models. The fraction of pulverization of each region was then scaled into a fraction of the overall rod. The pulverization fractions of each rod were averaged to calculate a best estimate core-wide FFRD susceptibility fraction.

The 95% confidence interval of each FFRD susceptibility was calculated using the standard error formulation,

$$U = 2\sqrt{\frac{p(1-p)}{n}}, \quad (2)$$

where  $U$  is the confidence interval,  $p$  is the best estimate FFRD susceptibility, and  $n$  is 242, the number of high-burnup rods analyzed in BISON. The results of this analysis are shown in Table 1 as best estimate-plus-confidence interval values. Note that these values represent the average FFRD susceptibility among *high-burnup* rods, not the entire core.

The full-core FFRD susceptibility is calculated by multiplying these percentages by the mass of fuel in each rod (2.162 kg) and the number of high-burnup rods (32,944). These predictions range from 0 kg to 5,392 kg, as shown in Fig. 14. The predictions show general agreement. The ranges predicted by the Turnbull/Strain rate and NRC RIL 2 mm/Chapman are the only ones that do not overlap.

The results presented in Table 1 and Fig. 14 represent the current best estimate of FFRD susceptibility for a full-size LWR experiencing an LBLOCA. The model could be improved by adding physical effects that were not included here. First, the BISON simulations did not include any transient FGR predictions. The inclusion of a transient FGR model could increase plenum pressure, which was linked to rod failure in Section 5. Second, the BISON simulations did not include the mechanical effects of spacer grids. Spacer grids put a compressive force on rods that counteract the tensile forces that cause ballooning. Including this force may reduce the number of rod failures. Finally, the RIL documents the impact of rupture opening. This was not considered in the evaluation, but quantifying the rupture opening is possible via Reference (Capps and Sweet, 2023) Therefore, this analysis assumes all material in the axial grid span is susceptible to dispersal without considering the effects of rupture size or location.

## 7. Conclusions and future work

A series of multiphysics simulations was used to predict the FFRD susceptibility of a full-power LWR during a postulated LBLOCA event of high-burnup fuel. First, VERA was used to model the full core during

**Table 1**  
FFRD susceptibility best estimates and confidence intervals for three FFRD models and two cladding failure models. These values represent the fraction of fuel susceptible to FFRD among high-burnup rods.

FFRD Model	Chapman Correlation (%)	Strain Rate Criterion (%)
NRC RIL 1 mm	$3.892 \pm 2.487$	$2.039 \pm 1.817$
NRC RIL 2 mm	$4.817 \pm 2.753$	$2.549 \pm 2.026$
Turnbull	$1.459 \pm 1.542$	$0.753 \pm 1.111$

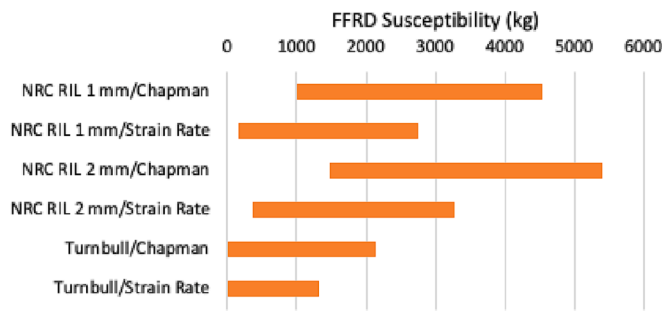


**Fig. 14.** Full-core FFRD susceptibility ranges for six pulverization/cladding failure model combinations.

steady-state operation of a high-burnup loading pattern. The VERA predictions were used to inform steady-state BISON models of a statistically representative set of fuel rods. The steady-state BISON results were used to benchmark a TRACE simulation of the LBLOCA event. Finally, the TRACE results were used to inform a set of transient BISON models. Over the course of these simulations, the number of rods was reduced from 32,944 high-burnup rods in VERA to 242 rods in the transient BISON simulation.

The transient BISON simulations included two models for cladding failure: the Chapman correlation and the strain rate criterion. These models were used to predict if, when, and where cladding burst could occur during the LBLOCA. Additional models were applied to predict the amount of fuel fragmentation in the regions surrounding the bursts and, therefore, the FFRD susceptibility. The margins of error of these predictions were also calculated to give estimated ranges for the FFRD susceptibility.

The FFRD susceptibility could be as high as 5,392 kg of fuel. However, it is important to note that this is a worst-case scenario built upon another worst-case scenario. Both cladding failure and pulverization models are meant to be conservative, and this amount of fuel dispersal is the highest value that was predicted among six model combinations. In addition, the postulated LBLOCA was also a worst-case accident scenario occurring at the end of the cycle, when burnups were highest. Such a perfectly timed accident is relatively unlikely.

This paper focuses primarily on the code coupling strategy and the FFRD susceptibility calculations. However, additional analyses were performed and are presented in more detail in two companion papers (Capps et al.; Wysocki et al., Unpublished manuscript). A comprehensive sensitivity and uncertainty analysis for the transient TRACE and BISON models is planned for future work.

In future work, several improvements can be made to this modeling approach to increase the prediction accuracy. First, more accurate decay heat generation rates can be calculated by VERA's ORIGEN module and implemented in BISON and TRACE. Second, a subchannel-scale LOCA calculation can be performed using the CTF code to assess localized TH effects on LOCA rod conditions. Third, additional physics such as mechanical effects of spacer grids and transient FGR can be included in the transient BISON simulations. In addition, the number of rods simulated could be increased to reduce the margins of error. Additional work can be performed to better validate cladding failure, fuel pulverization, and other models used in VERA, TRACE, and BISON to reduce the inherent uncertainties of the models' predictions. Finally, the implementation of mechanistic models can help researchers better understand cladding and fuel behavior during the transient and better identify margin to burst and FFRD susceptibility.

## CRediT authorship contribution statement

**Ian Greenquist:** Methodology, Software, Formal analysis, Writing – original draft, Writing – review & editing, Visualization. **Aaron Wysocki:** Methodology, Software, Formal analysis, Writing – original

draft, Writing – review & editing, Visualization. **Jake Hirschhorn:** Methodology, Software, Formal analysis, Writing – original draft, Writing – review & editing, Visualization. **Nathan Capps:** Conceptualization, Writing – original draft, Writing – review & editing, Supervision, Project administration, Funding acquisition.

## Declaration of Competing Interest

The authors declare that they have no known competing financial interests or personal relationships that could have appeared to influence the work reported in this paper.

## Data availability

Data will be made available on request.

## Acknowledgements

This work was supported by the Advanced Fuels Campaign (AFC) of the US Department of Energy Office of Nuclear Energy. This work would not have been possible without the collaboration and contributions of Southern Nuclear Company. The Nuclear Energy Advanced Modeling and Simulation (NEAMS) Program of the US Department of Energy Office of Nuclear Energy supported the analysis herein. The authors would like to express appreciation to Jacob Gorton, Aaron Graham, Andrew Nelson, and Christian Petrie of ORNL for their reviews and feedback of this paper. Lastly, this research made use of the High-Performance Computing Center at INL, which is supported by the Office of Nuclear Energy of the US Department of Energy and the Nuclear Science User Facilities under contract No. DE-AC07-05ID14517.

## References

- Bajorek, S., Gavrillas, M., Gingrich, C., Han, J., Hogan, K., Kelly, J., Krotiuk, W., Lauben, N., Lu, S., Murray, C., Odar, F., Rhee, G., Rubin, M., Smith, S., Staudenmeier, J., Uhle, J., Wang, W., Welter, K., Han, J., Klein, V., Burton, W., Danna, J.A., Jolicoeur, J., Basu, S., Madni, I., Marshall, S., Velazquez, A., Kadambi, P., Bessette, D., Bennet, M., Salay, M., Ireland, A., Macon, W., Eltawila, F., Guan, Y., Ebert, D., Du, D., Fang, T., He, W., Straka, M., Palmrose, D., Jones, Mahaffy, J., Trujillo, M., Jelinek, M., Lazor, M., Hansell, B., Watson, J., Meholic, M., Aktas, B., Amoruso, C., Barber, D., Bolander, M., Caraher, D., Delfino, C., Fletcher, D., Larson, D., Lucas, Mortensen, G., Palazov, V., Prelewicz, D., Shumway, R., Tompot, R., Wang, D., Spore, J., Boyack, B., Dearing, S., Durkee, J., Elson, J., Giguere, P., Johns, R., Lime, J., Lin, J.-C., Pimentel, D., Downar, T., Miller, M., Gan, J., Joo, H., Xu, Y., Kozlowski, T., Jung Lee, D., Herrero, R., Jeong, J.H., Huh, C.W., Shin, A.D., TRACE V5.0 Theory Manual: Field Equations, Solution Methods, and Physical Models, (n.d.). <https://www.nrc.gov/docs/ML1200/ML120060218.pdf> (accessed November 23, 2022).
- Bales, M., Chung, A., Corson, J., Kyriazidis, L., 2021. Interpretation of Research on Fuel Fragmentation, Relocation, and Dispersal at High Burnup. U.S. Nuclear Regulatory Commission, Rockville, Maryland <https://www.nrc.gov/docs/ML2131A145.pdf>.
- Capps, N., Greenquist, I., Wysocki, A., Hirschhorn, J., Multiphysics Analysis of Fuel Fragmentation, Relocation, and Dispersal Susceptibility-Part 2: High Burnup Steady State Operating and Fuel Performance Conditions, Annals of Nuclear Energy. (Unpublished manuscript).
- Capps, N., Sweet, R., Wirth, B.D., Nelson, A., Terrani, K., 2020. Development and demonstration of a methodology to evaluate high burnup fuel susceptibility to pulverization under a loss of coolant transient. Nucl. Eng. Des. 366, 110744.
- Capps, N., Sweet, R., 2023. Model for determining rupture area in Zircaloy cladding under LOCA conditions. Nucl. Eng. Des.
- Capps, N., Wysocki, A., Godfrey, A., Collins, B., Sweet, R., Brown, N., Lee, S., Szewczyk, N., Hoxie-Key, S., 2020. Full Core LOCA Safety Analysis for a PWR Containing High Burnup Fuel. Oak Ridge National Laboratory, Oak Ridge, Tennessee.
- Capps, N., Wysocki, A., Godfrey, A., Collins, B., Sweet, R., Brown, N., Lee, S., Szewczyk, N., Hoxie-Key, S., 2021. Full core LOCA safety analysis for a PWR containing high burnup fuel. Nucl. Eng. Des. 379, 111194 <https://doi.org/10.1016/j.nucengdes.2021.111194>.
- Di Marcello, V., Schubert, A., van de Laar, J., Van Uffelen, P., 2014. The TRANSURANUS mechanical model for large strain analysis. Nucl. Eng. Des. 276, 19–29. <https://doi.org/10.1016/j.nucengdes.2014.04.041>.
- El-Wakil, M.M., Nuclear Heat Transport, First Thus edition, Amer Nuclear Society, La Grange Park, Ill, 1978.
- Erbacher, F.J., Neitzel, H.J., Rosinger, H., Schmidt, H., Weirh, K., Burst Criterion of Zircaloy Fuel Claddings in a Loss-of-Coolant Accident, in: Zirconium in the Nuclear Industry, ASTM International, 1982: pp. 271–282.
- Powers, D.A., Meyer, R.O., 1980. Cladding Swelling and Rupture Models for LOCA Analysis. U.S. Nuclear Regulatory Commission, Washington, DC.
- Rearden, B.T., Jessee, M.A., Scale Code System, Oak Ridge National Laboratory, Oak Ridge, Tennessee, 2018. <https://info.ornl.gov/sites/publications/Files/Pub107333.pdf> (accessed October 26, 2022).
- Reventos, F., Perez, M., Batet, L., Pericas, R., 2008. Simulation of a LBLOCA in ZION Nuclear Power Plant – BEMUSE Phase IV Report. Organisation for Economic Co-operation and Development, Paris, France <https://arpi.unipi.it/handle/11568/907208> (accessed October 27, 2022).
- Salko, R., Avramova, M., Wysocki, A., Toptan, A., Hu, J., Porter, N., Blyth, T., Dances, C., Gomez, A.C., Jernigan, J., Kelly, A., Abarca, CTF Theory Manual Version 4.2, Consortium for Advanced Simulation of LWRs, Oak Ridge, Tennessee, 2020.
- Turnbull, J.A., Yagnik, S.K., Hirai, M., Staicu, D.M., Walker, C.T., 2015. An assessment of the fuel pulverization threshold during LOCA-type temperature transients. Nucl. Sci. Eng. 179 (4), 477–485.
- Turner, J.A., Clarno, K., Sieger, M., Bartlett, R., Collins, B., Pawlowski, R., Schmidt, R., Summers, R., 2016. The Virtual Environment for Reactor Applications (VERA): Design and architecture. J. Comput. Phys. 326, 544–568.
- US NRC, 50.46 Acceptance criteria for emergency core cooling systems for light-water nuclear power reactor, (2021). <https://www.nrc.gov/reading-rm/doc-collections/cfr/part050/part050-0046.html> (accessed October 27, 2022).
- Williamson, R.L., Hales, J.D., Novascone, S.R., Pastore, G., Gamble, K.A., Spencer, B.W., Jiang, W., Pitts, S.A., Casagrande, A., Schwen, D., Zabriskie, A.X., Toptan, A., Gardner, R., Matthews, C., Liu, W., Chen, H., 2021. BISON: a flexible code for advanced simulation of the performance of multiple nuclear fuel forms. Nucl. Technol. 207, 954–980. <https://doi.org/10.1080/00295450.2020.1836940>.
- Wysocki, A., Capps, N., Greenquist, I., Hirschhorn, J., Multiphysics Analysis of Fuel Fragmentation, Relocation, and Dispersal Susceptibility-Part 3: Thermal Hydraulic Evaluation of Large Break LOCA Under High Burnup Conditions, Annals of Nuclear Energy. (Unpublished manuscript).